Solar Energy Materials & Solar Cells 230 (2021) 111275

Contents lists available at ScienceDirect

Solar Energy Materials and Solar Cells

journal homepage: www.elsevier.com/locate/solmat

Adaptive covers for combined radiative cooling and solar heating. A review of existing technology and materials

Roger Vilà, Ingrid Martorell, Marc Medrano *, Albert Castell

Sustainable Energy, Machinery and Buildings (SEMB) Research Group, INSPIRES Research Centre, Universitat de Lleida, Pere de Cabrera s/n, 25001, Lleida, Spain

ARTICLE INFO

Keywords:
Radiative cooling
Solar thermal collection
Renewable energy
Adaptive cover
Convection suppression

ABSTRACT

Radiative cooling is a promising technology for space cooling. This technology can be combined with solar heating applications, enabling the production of both energy demands –heat during daytime and cold during nighttime– in a single device; thus, reducing the non-renewable primary energy consumption for space conditioning and domestic hot water. Radiative cooling and solar heating appear in different wavelength ranges, 8–14 μm and 0.25–2.5 μm respectively, thus the device must be able to switch between ranges in each mode. An adaptive cover placed on top of the radiator/absorber can provide this switch by combining materials with suitable optical properties for each mode. Another effect derived from the usage of covers is the reduction of convective heat losses, enhancing the performance of the device. This paper aims to review the existing materials used in solar collectors, and radiative coolers as well as available smart materials used in other fields for its potential use as adaptive covers for combined radiative cooling and solar heating applications.

1. Introduction

Energy transformation is indispensable for the functioning of today's societies; almost everything we do is possible due to the human capacity to extract energy from other sources to take advantage of it in our favor. Social and economic transformations resulting from Industrial Revolutions were a consequence of the replacement of energy sources available at the time by coal and later by oil, natural gas and electricity. Demand for the current model of energy consumption continues growing year after year – driven by population and industrial growth, as well as a rising in the living standards – while fossil resources still account for the 70% of the total of that growth [1].

One of the problems arising from the current energy model is the high volumes of greenhouse gases emitted into the atmosphere. The contribution of these gases to climate change as a result of human activity has reached a consensus among the scientific community [2] and global environmental awareness is currently increasing in society.

This challenge is being considered in recent public policies. In the case of the European Union it is determined to become an economy based on a low energy consumption, stable and secure, competitive, locally produced and sustainable. This is expressed in Directive 2009/28/CE on the promotion of energy from renewable resources [3], Directive 2018/844 [4] –amending Directive 2010/31/UE, concerning energy efficiency of buildings, and Directive 2012/27/EU on energy efficiency–, and recommendations 2019/786 on the renovation of buildings [5]. Moreover, Project Europe 2030 [6], which replaces the Europe 2020 Project, sets out three key goals by 2030: (a) a reduction of at least 40% of greenhouse gas emissions with respect to 1990 values, (b) a share of at least 32% in renewable energy and (c) an improvement of at least 32.5% in energy efficiency.

The above mentioned relates to the high potential for reduction in energy consumption in buildings. In the EU, energy consumption in buildings is estimated to account for 40% of the total energy consumption, while accounting for 36% of CO_2 emissions [7]. The demand in residential sector is mostly covered by natural gas (36%) and electricity (24.1%), while renewables only account for 17.5%. Specifically, 64.1% of the total consumption in buildings is dedicated to space heating, 14.8% to Domestic Hot Water (DHW), and 0.3% to space cooling; accounting for almost 80% of the energy consumed [8]. As for space heating, the energy sources are quite diverse: natural gas dominates, but renewable sources already account for more than 20% and in a smaller proportion in DHW. According to data from Eurostat, space cooling is still entirely achieved by electricity consumption [8].

Currently, solar heating is a renewable technology which already has commercial applications in the field of energy production of heat and/or DHW. Cold generation is relegated to the use of nonrenewable air conditioning units which operate through compression or absorption

* Corresponding author.
E-mail addresses: roger.vila@udl.cat (R. Vilà), ingrid.martorell@udl.cat (I. Martorell), marc.medrano@udl.cat (M. Medrano), albert.castell@udl.cat (A. Castell).

https://doi.org/10.1016/j.solmat.2021.111275
Received 13 January 2021; Received in revised form 28 June 2021; Accepted 29 June 2021

Nomenclature

A	Radiator/Absorber surface (m^2)
$E_b(T)$	Power absorbed/emitted by a blackbody surface at temperature T (W)
$E(T)$	Power absorbed/emitted by a surface at temperature T (W)
h_c	Film coefficient ($W/m^2 \cdot K$)
k_{air}	Thermal conductivity of air (W/m·K)
k_s	Thermal conductivity of the surface (W/m·K)
L	Characteristic length (m)
P	Perimeter of the surface (m)
Pr	Prandtl Number (−)
Q_a	Absorbed infrared radiation from atmosphere (W)
Q_{cond}	Conduction heat power (W)
Q_{conv}	Convective heat power (W)
Q_{net}	Net balance radiation power (W)
Q_s	Infrared radiation power emitted by a radiative surface (W)
Q_{sun}	Incident solar radiation power (W)
Re	Reynolds Number (−)
T_a	Ambient temperature (K)
T_s	Surface temperature (K)
∇T	Temperature gradient (K)
σ	Stefan-Boltzmann's constant: $5.6704 \cdot 10^{-8}$ ($W/m^2 \cdot K^4$)
ε	Emissivity (−)
ε_s	Surface emissivity (−)
ε_{sky}	Effective sky emissivity (−)
τ	Transmittance (−)
τ_{atm}	Transmittance in the atmospheric window's range (−)
τ_{sol}	Transmittance in the solar range (−)
ρ	Reflectivity (−)
ρ_{atm}	Reflectivity in the atmospheric window's range (−)
ρ_{sol}	Reflectivity in the solar range (−)
α	Absorptivity (−)
α_{atm}	Absorptivity in the atmospheric window's range (−)
α_{sol}	Absorptivity in the solar range (−)

processes. Literature points out that radiative cooling can become a feasible possibility for renewable cooling production for space conditioning purposes [9,10].

Radiative cooling is a process by which a surface reduces its temperature by emitting thermal radiation towards the outer space taking advantage of the infrared atmospheric window transparency in the 8–14 μm range. Initially radiative cooling occurred at night only, as the energy balance during the day results in energy gains by solar radiation; however, with the development of new photonic materials and metamaterials, daytime surface cooling has been achieved [11–13]. Under clear sky conditions radiative cooling is maximized [14]. Ambient conditions and optical properties of materials play a role on the total performance of radiative cooler devices; currently they present low cooling rates (between 20 and 80 W/m^2 on average with peaks at 120 W/m^2) [15]. Total cooling rates are influenced by conduction and convection heat gains. In order to achieve higher cooling rates, various authors have proposed the use of convective barriers which separate the emitting surface from the environment, cutting down convective heat exchanges [16] and enabling surface cooling below ambient temperature [17,18].

The operation of radiative cooling is totally opposite to that of solar heating, since it occurs at different times of the day and in a different wavelengths range. Nevertheless, both functions are analogous so that combination of both functionalities has been proposed by various authors [15,19,20,21], thus enabling the production of both energy demands (heat and cold)– in a single device. As stated by Vall et al. [15], the use of both technologies may substantially reduce the non-renewable primary energy consumption for space conditioning and domestic hot water and it will make the investment more cost-effective. The payback of this technology could be of a period of 8 years [22].

Vall et al. simulated a mixed solar collector/radiative cooling system in order to evaluate the potential coverage of the demand in different building typologies and climates. The results showed that in five of the studied cities (representing five different climates in the world) it could achieve a minimum coverage of 25% of cooling and 75% of DHW in residential and hotel building typologies. In literature there is not a consensus name for this combined system: The authors named this device *Radiative Collector and Emitter (RCE)*. For the sake of simplicity, this paper also refers to it as RCE.

RCE works in two differenced modes in different wavelengths ranges: nighttime radiative cooler emits in the 3–25 μm range (long wave) while daytime collector absorbs solar radiation in the 0.2–3 μm range and blocks long waves. This will be further discussed in section 2; however, the key is to know that RCE must have different optical properties which depend on the working mode.

To achieve this dual function two strategies have been identified: (1) to place an adaptive cover with selective transmittances on top of a black surface. The black surface absorbs/emits all the radiation while the cover filters the desired wavelengths. Covers, at the same time, can diminish the effects of convective exchanges, named convective covers. There are two typologies of adaptive covers: an exchangeable cover [23] which uses different materials depending on each working mode, or a smart material cover which is able to switch its optical properties depending on the working mode. Alternatively, (2) a second strategy is to use a selective surface, which controls the emissive/absorbance properties of the surface in different wavelengths ranges. As it has been previously stated, metamaterials with selective emissivity/absorptivity have already been proposed for all day radiative cooling applications [11–13]. However, up until this point, more complex metamaterials for combined radiative cooling and solar heating applications have not been investigated. These selective surfaces could also make use of a cover to diminish the effects of convection.

This paper puts the focus on the first mentioned strategy. Different reviews have been published on radiative cooling technology, including those by Lu et al. [24], Vall et al. [25], Nwaji et al. [26] and Zhao et al. [27]. Other reviews have focused specifically on materials for radiative cooling purposes, such as Granqvist and Niklasson [28], Ko [12] or Santamouris and Feng [9], placing its focus on emitter surfaces. However, to our knowledge, no revision of materials used in convective suppression applied to radiative cooling and solar heating has been presented. In this paper we review the different approaches presented in literature for RCE covers which allow the combination of both radiative collectors and emitters, while reducing the negative convection gains.

2. Background

2.1. Solar and infrared range

All the bodies being at a temperature above absolute zero are continuously radiating thermal energy. The energy emitted per unit surface area is according to Boltzmann's law (eq (1)). The amount of energy emitted from a surface, at a given wavelength, will depend on the material and conditions of the surface as well as the temperature of the surface. For a blackbody surface, the energy absorbed and emitted is maximum (Eq. (2)).

$$E(T) = \varepsilon\sigma T^4 \quad (1)$$

$$E_b(T) = \sigma T^4 \quad (2)$$

The Sun, being at near 5800 K, is considered to be a black body emitting shortwave radiation between the ultraviolet and the near-infrared band with its peaks falling in the visible range; collectors absorb energy within these wavelengths. Then again, cold bodies at ambient temperature (~300K) emit longwave radiation in the infrared band towards the outer space, which is at 3K [29]. Due to this large difference in temperatures, space becomes an energy sink. This process is possible due to the high transparency of the atmosphere at 0.3–3, 3.2–4.8, 8–14 and 16–23 μm wavelengths (Fig. 1). These transparent ranges are known as atmospheric windows. In the 8–14 μm range of wavelengths, atmospheric window matches a high portion of the infrared energy radiated by the bodies, enabling a temperature reduction.

It is noted that each mode of the RCE operates in different wavelengths ranges. For an RCE cover, during heating mode, it is desired to allow all the solar radiation to pass through the cover while blocking the infrared radiation. During cooling mode, it is desired to allow all the 8–14 μm radiation emitted by the surface to pass through the cover. Table 1 summarizes the optical properties of and ideal cover of an RCE.

2.2. Nonradiative heat gains

When a surface is not in an isolated environment, it is exposed to the following energy exchanges (Fig. 2):

1. Incoming short wavelength (0.3–2.5 μm) solar radiation which is absorbed by the surface. This energy flux is only present during daytime.
2. Infrared radiation emitted by the atmosphere and absorbed by the surface.
3. Infrared radiation emitted by the surface to the atmosphere.
4. Thermal gains/losses by exchange with the surrounding air or adjacent solids in the form of convection or conduction, respectively.

The total energy exchanged in the form of heat can be expressed according to Eq. (3). Due to the small value of σ, at low temperatures the effect of radiation is negligible compared to the conduction and convection effects. When temperature increases, due to the effect of T^4, the contribution of radiation is dominant. RCE systems at near ambient temperatures fall in a range where the three effects have to be considered.

When the surface temperature (T_s) is different from the ambient temperature (T_a), nonradiative exchanges with the environment (conduction and convection) exist. During nighttime radiative cooling applications, if the cooler is designed to work at $T_s > T_a$, it would benefit from convective and conductive heat exchanges [31] while for $T_s < T_a$, nonradiative exchanges would reduce the total performance of the RCE [32]. In contrast, during daytime solar heating applications,

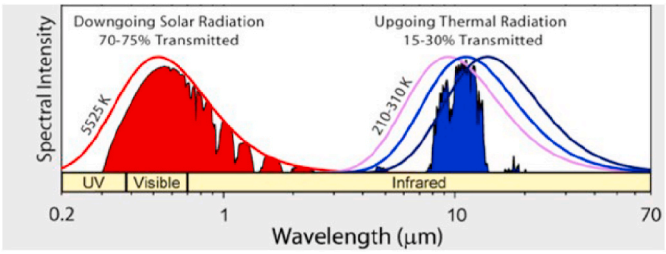

Fig. 1. Solar radiation (red) and radiation through the atmospheric window (blue). Modified from Ref. [30]. (For interpretation of the references to color in this figure legend, the reader is referred to the Web version of this article.)

Table 1
Ideal optical properties of a RCE cover.

	Solar Spectrum		Atmospheric Window	
	Transmittance	Emittance	Transmittance	Emittance
Heating mode	100%	0%	0%	0%
Cooling mode	–	–	100%	0%

nonradiative heat exchanges would enhance the overall performance of the RCE when $T_s < T_a$ while it would be reduced when $T_s > T_a$, the most usual situation. For an RCE with overambient daytime temperatures and subambient nighttime temperatures, energy will be maximum when the convection and conduction gains are minimal (Eq. (4)).

$$Q_{net} = Q_s(T_s) - Q_a(T_a) + Q_{sun}(T_{sun}) - Q_{cond} - Q_{conv} \quad (3)$$

$$Q_{net} = A \cdot \sigma \cdot \varepsilon_s \left(T_s^4 - \varepsilon_{sky} T_a^4\right) + Q_{sun}(T_{sun}) \quad (4)$$

Conduction heat gains are the consequence of thermal energy exchanging processes between bodies in contact at different temperatures (Eq. (5)). In the case of a radiative cooler, heat gains will appear on the emitter/absorber's walls and can be minimized with thermal insulation.

$$Q_{cond} = -k_s \cdot A \cdot \nabla T \quad (5)$$

Convection is a thermal energy transfer between areas of the same fluid at different temperatures through the movement of the molecules inside these areas. In the case of the radiative cooler, this movement occurs between the air particles in contact with the surface at a lower temperature and the air particles at room temperature. The convective heat gains can be expressed with Eq. (6).

$$Q_{conv} = h_c \cdot A \cdot (T_s - T_a) \quad (6)$$

The convection heat transfer coefficient on a flat plate can be expressed based on the Nusselt number (Eq. (7)) which takes into account both free and forced convection effects. Different authors have fitted empirical correlations to convection heat transfer coefficient as a function of wind speed, increasing as the velocity increases [33]. Table 2 shows the approximations used by authors in different contexts.

$$h_c = \frac{Nu \cdot k_{air}}{L} \quad (7)$$

Zhao et al. [18] experimentally studied the effects of wind speed on radiative surface performance. The results showed that the difference in temperatures between the circulating water and the environment decreased from 7 °C to 4.3 °C (Fig. 3) due to a change of wind speed when the convective cover was removed.

3. Exchangeable adaptive cover

An exchangeable adaptive cover concept can be viewed as a combination of two different covers that can be swapped, one for solar heating mode and the other for radiative cooling mode, providing low spectral transmittance in the infrared band and high spectral transmittance in the solar range during the daytime solar collection mode, and high spectral transmittance in the 8–14 μm wavelength range during nighttime radiative cooling mode.

Commercial flat plate solar collectors are provided with low emissivity glass covers with the aim of letting solar radiation pass through, while preventing heat loss to the environment. Moreover, thanks to the very low transmittance on the whole infrared (IR) spectrum of this glass, it blocks thermal radiation to escape from the surface while acting as a convective suppressor for the collector, enhancing the total performance. Glass by itself is not a good candidate for RCE applications, as it would prevent radiative cooling at night. Alternatively, polyethylene film has high transmittance both in the infrared and the solar spectrum (Table 3), allowing radiative cooling during night. Glass can be placed

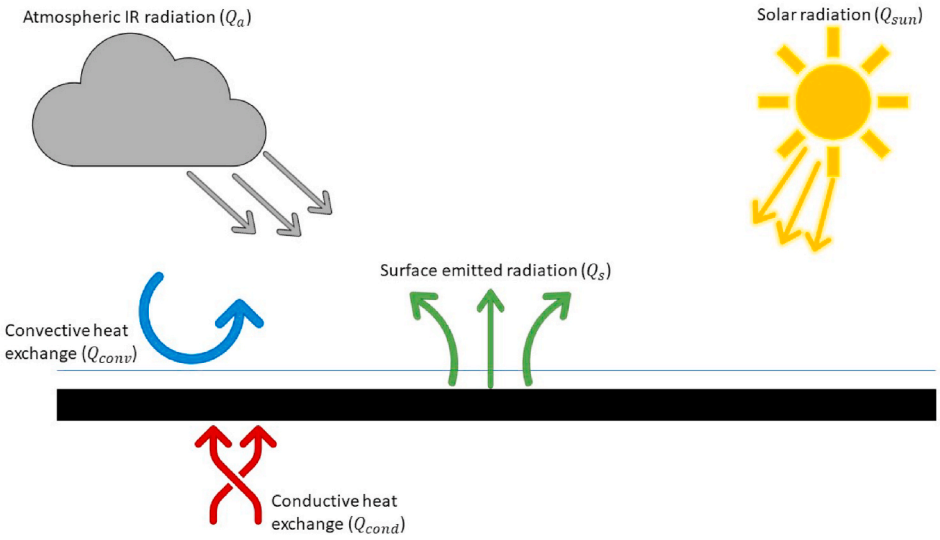

Fig. 2. Thermal exchanges between the radiative surface and its surroundings.

on top of polyethylene during daytime to improve the RCE performance and be removed during nighttime. Vall et al. [15] proposed to slide the glass on top of polyethylene films (Fig. 4), enabling the automation of the process. Liu et al. [22] alternatively designed a combined device made of 10 μm polyethylene film, a porous cooling material with near unity infrared emissivity in the 8–13 μm range, aluminum conductor substrate, providing heat conductivity, and a solar absorbing material (Fig. 5) coated with chromium plating (solar absorptivity of 95%). Radiative cooling was achieved on one layer of the device while solar collection was done on the other layer of the device; the switching between modes was achieved with a rotating shaft.

In solar collection applications glass is widely used [42,43] and has become the standard material. In contrast, there is not yet a standard material in radiative cooling applications and it is still a subject of study.

3.1. Convective covers based on polymers

The main feature for convective covers, also named windscreens, in radiative cooling applications is its high transmittance in the far-infrared (FIR) spectrum. Due to this characteristic, windscreens are placed on top of emitters, separating the radiator from the environment conditions. In 1975, Johnsons [16] investigated the use of a 0.0005 in (0.0127 mm) cover of fluorinated ethylene propylene (FEP or Teflon) film. Film was protected against water attack and structurally reinforced with aluminum ribs. The author measured a transparency of 70%, but he stated that the film was too thin to withstand environmental conditions. Orel et al. [44] used a polyester foil with a thickness of 50 μm. Authors only affirmed that it was transparently enough for infrared radiation to cover an aluminum radiator.

Despite the two materials described above, the material most commonly used as a windscreen has been polyethylene due to its high transmittance in the atmospheric window (Fig. 6). To reduce conductive and convective heat exchanges, Bartoli et al. [45] built in 1977 an insulating styrophoam box covering the radiator with a polyethylene sheet of 50 μm thickness on top; although it was presented to have almost ideal transparency, it had quite low mechanical properties and, under high humidity conditions, it showed moisture condensation, decreasing the optical properties.

Tsilingris [46] studied the infrared transmittances of various polymers for their utilization as a suppressor for the convective losses/gains in solar collector/emitting surfaces. Of the ten samples analyzed – plexiglass, fiberglass, polycarbonate, polyethylene, polypropylene, tedlar, mylar, kapton and vinyl – Tsilingris sentenced that polyethylene and polypropylene had the highest transmission, making them suitable for radiative cooling applications; while fiberglass, kapton and mylar showed the lowest coefficients, being suitable for solar collector applications.

Leroy et al. [47] used a polyethylene aerogel as a cover: it showed low thermal conductivity, high transmittance in the atmospheric window (0.799) and high reflectance of solar radiation (0.922). This offers the possibility to achieve daytime radiative cooling. Raman et al. [17] covered a photonic solar reflector and thermal emitter with a 12.5 μm thick LDPE to obtain daytime radiative cooling. The system, which had a 97% reflectance in the solar band and high emittance in the longwave range, was able to cool to 4.9 °C below ambient. In the last decade, various authors have used polyethylene foils –both high density polyethylene (HDPE) and low density polyethylene (LDPE)– as convective windscreen materials combined with new structures such as crystals, metamaterials and photonic crystal, which serve as emitting surface, to achieve daytime radiative cooling. Xu et al. covered with polyethylene a new crystal with 87% emittance in the atmospheric window and 88% solar reflective [48]. Zhao et al. combined a polymer metamaterial film with a PE cover achieving a difference of 10 °C between circulating water and ambient temperature under solar radiation [18]. Anodic aluminum oxide covered with PE presented cooling power of 64 W/m^2 and cooling temperatures of 2.6 °C below ambient [49].

Because of the optical properties and also the low cost and availability of polyethylene, it has been tested in mixed heating and cooling applications. In 1987, Matsuta et al. [19] used a selective solar heating/radiative cooling surface covered with a polyethylene film to prevent convective exchanges achieving maximum values of 610 W/m^2 in collection mode and 51 W/m^2 in radiative mode. Long et al. [21] developed a composite surface made of silica micro-grating and p-doped Si, covered with polyethylene, to enable both solar collection and radiative cooling. Hu et al. developed a selective surface highly emitting/absorbing in both the solar range and atmospheric window band covered with a PE convective cover; the system had a cooling power of 50.3 W/m^2, under clear night conditions, and a solar collector efficiency of 62.7% [20,50]. A combined radiative cooling/solar heating system based on water circulating under a black surface –protected with LDPE film– presented a daily thermal efficiency between 26.8 and 40.7% and a cooling efficiency of 58.3% [51].

Radiative cooling simulations also make use of polyethylene covers in the models. Mihalakakou et al. [41] modeled, using TRNSYS, the performance of a radiative cooling system in a building. The system consisted of a stainless steel radiative cooler covered with a

Table 2
Summary of convection coefficient correlations.

Reference	Coefficient correlation	Units	Characteristic dimensions in the study	Observations and Applications
[18]	$h_c = 8.3 + 2.5v$	W/m^2K	A = 0.58 m × 0.58 m	Radiative cooler without windscreen 0 < v < 8 m/s
[18]	$h_c = 2.5 + 2v$	W/m^2K	A = 0.58 m × 0.58 m	Radiative cooler with windscreen 0 < v < 8 m/s
[34]	$h_c = 5.7 + 3.8v$	W/m^2K	L = 2.9	Small flat plate solar collectors
[35]	$h_c = 2.8 + 3v$	W/m^2K	A = 2 m × 1 m	Thermal simulation of solar energy systems
Berdahl and Clark quoted in [36]	$h_c = 0.8$	W/m^2K	–	$T_s < T_a$ Free convection (v < 0.076 m/s)
Berdahl and Clark quoted in [36]	$h_c = 3.5$	W/m^2K	–	Ts > Ta Free convection (v < 0.45 m/s)
Berdahl and Clark quoted in [36]	$h_c = 0.054 \cdot Re^{0.8} Pr^{0.33} \cdot k_S/L$	W/m^2K	–	Turbulent flow
Berdahl and Clark quoted in [36]	$h_c = 1.8 + 3.8v$	W/m^2K	–	Turbulent flow (1,3 < v < 4,5 m/s)
[37]	$h_c = 5.7 + 3.8v$	W/m^2K	L < 0.5 m	–
Sparrow (1979) quoted in [38]	$h_c = 4.6v^{0.5} L^{-0.5}$	W/m^2K	$L = \frac{4 \cdot A}{P}$	Horizontal flat plate
Lunde (1980) quoted in [38]	$h_c = 4.5 + 2.9v$	W/m^2K	–	–
[39]	$h_c = 9.4v^{0.5}$	W/m^2K	–	Fitted equation to experimental data
[40]	$h_c = 0.6 + 3.5v^{0.5}$	W/m^2K	–	Without windscreen
[40]	$h_c = 0.5 + 1.2v^{0.5}$	W/m^2K	–	Single polyethylene layer windscreen
[40]	$h_c = 0.3 + 0.8v^{0.5}$	W/m^2K	–	Double windscreen
[41]	$h_c = 3.1 + 4.1v$	W/m^2K	A = 14 m × 7 m	Forced convection 0.1 < v < 2 m/s
[41]	$h_c = 5.7 + 3.8v$	W/m^2K	A = 14 m × 7 m	Without windscreen v < 4 m/s
[41]	$h_c = 7.3v^{0.8}$	W/m^2K	A = 14 m × 7 m	Without windscreen v > 4 m/s
[41]	$h_c = 0.5 + 1.2v^{0.5}$	W/m^2K	A = 14 m × 7 m	Single polyethylene layer windscreen

polyethylene film of 60–100 μm of thickness. Daily energies varied between 29.7 and 55.8 W h/m^2 under clear sky and between 26.7 and 44.9 W h/m^2 for a cloudy day.

In 1998, Al-Nimr et al. [52] developed a mathematical model which described the dynamic thermal behavior of a radiative cooling system consisting of a black surface and a polyethylene thin film of 40 μm on top. This model assumed that the polyethylene cover had perfect radiative properties. The analytical solution showed lower outlet temperature predictions compared to experimental results.

Due to the transparency of polyethylene in the solar range, it has not only been used in radiative cooling and RCE applications but also in photovoltaic/radiative cooling mixed systems (PV/RC) for the combined generation of electricity during daytime and cold during night. Zhao et al. were able to achieve 12.7 °C reduction below ambient nighttime temperature with an average electrical conversion efficiency of 12.4% [53]. The PV/RC performance is strongly dependent on climate areas and seasons [54–56].

3.1.1. Pigmented covers

Andretta et al. [65] in 1981 made a lowcost cover blending in two layers of polyethylene with commercial standard pigments, such as TiO_2 and carbon black, with the aim of reflexing part of the solar radiation while absorbing the rest through the carbon black. The authors achieved subambient temperatures under these films even during daytime. Single layers of polyethylene pigmented with TiO_2 were also studied by Niklasson and Erikson [66]. Authors concluded that these covers were able to achieve radiative cooling for more than 19 h of the day. Using hot pressing technique with small particles of TiO_2 (diameter of 60 nm) into two polyethylene foils Mastai et al. [67] could obtain transmittance in the atmospheric window regions of 0.54–0.765 and high solar reflectances (Table 4).

Zinc based pigments blended into two polyethylene foils have also been used as convective covers. The performance of polyethylene with different pigments, including ZnS, ZnSe, ZrO_2 and ZnO where studied by Nilsson et al. [68]. Results showed that ZnS is the best pigment among the others to be used in selective covers [68–71].

3.1.2. PbS, PbSe and Te deposited films

PbS, PbSe and Te deposited on polyethylene films can also act as shields. Dobson et al. [71] compared different films produced by chemical solution deposition (CSD) techniques: in particular they produced PbSe and PbS films on polyethylene films and on ZnS and ZnO pigmented polyethylene films. The films showed a variety of optical properties based on the deposition parameters: in the case of the PbS, the films deposited from potassium nitrilotriacetate (NTA) showed high transmittance in the atmospheric window (Table 5) while with trisodium citrate (TSC) depositions the transmittance was slightly lower. In the case of the PbSe, transmittance in the atmospheric range was lower, as well as the reflectance in the solar spectrum due to the NTA baths. PbS films presented high absorption in the solar range. Authors also studied the behavior of PbS semiconductor laminates deposited on pigmented polyethylene with ZnS and ZnO. Transmittance values in the solar range were very low (0.04 and 0.03), while absorption values in this range were higher than 0.62. Engelhard et al. [72] developed an easy method to deposit Te films on a polyethylene substrate –pretreated with $KMnO_4$– using the room temperature decomposition of electrochemically

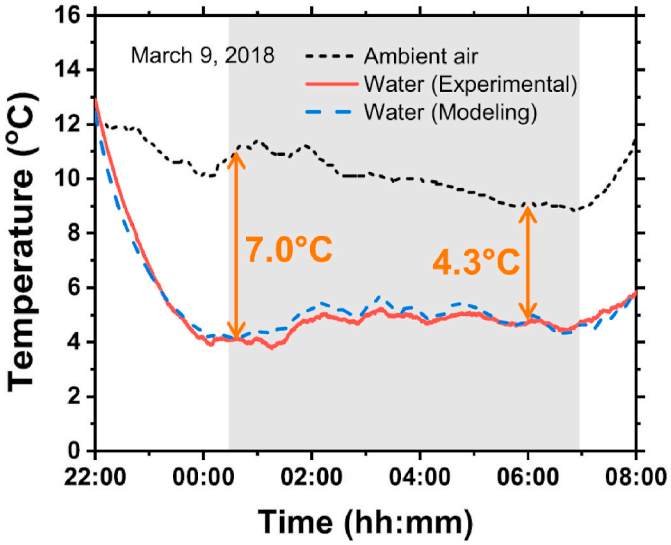

Fig. 3. Experimental temperatures obtained from a radiative cooling test, showing the effect of wind. During the colored grey period PE windscreen was not used on top of the emitting surface [18].

Table 3
Summary of transmittances of polymeric covers.

Cover material	Reference	Thickness	τ_{atm}	τ_{sol}	Application	Comment
Teflon	[16]	127 μm	~0.7	–	RC	–
LDPE	[17]	12.5 μm	–	–	Daytime RC	–
LDPE	[20,50,55]	20 μm	0.83[a]	0.85[1]	SH/RC	–
LDPE	[54]	6 μm	0.87[1]	0.89[1]	PV/SH/RC	–
LDPE	[46,62]	6 μm	0.87	0.89	SH/RC	–
LDPE	[53]	–	High	High	RC/PV	–
LDPE	[57]	20 μm	–	–	Daytime RC	–
LDPE	[58]	–	–	–	Daytime RC	–
PE	[19]	30 μm	0.86[b]	0.85[1]	SH/RC	–
PE	[46]	130 μm	0.79[1]	–	–	–
PE	[46]	50 μm	0.88[1]	0.87[1]	SH/RC	–
PE	[48]	–	–	–	Daytime RC	–
PE	[49]	50 μm	–	–	Daytime RC	–
PE	[52]	40 μm	High	–	RC	–
PE	[59]	50 μm	0.72	–	RC	New film
			0.69			5 days exposition
			0.57			30 days exposition
			0.42			100 days exposition
PE	[60]	50 μm	0.74[1]	–	RC	–
PE	[61]	1 μm	0.92	–	SH/RC	–
PE	[62]	Ø150 μm	0.872	–	RC	Fibermesh cover
PE	[63]	30 μm	0.85	–	RC	–
PE	[64]	–	0.92	<0.45	Daytime RC	–
PE aerogel	[47]	6 mm	0.80	0.11	Daytime RC	–
Polyester	[44]	50 μm	High	–	RC	–
Polycarbonate	[46]	1.22 mm	0.06[1]	–	–	–
Kapton	[46]	130 μm	0.08[1]	–	–	–
Mylar	[46]	130 μm	0.05[1]	–	–	–
PP	[46]	130 μm	0.50[1]	–	–	–
Plexiglass	[46]	1.52 mm	0.01[1]	–	–	–
Vinyl	[46]	125 μm	0.21[1]	–	–	–
Fiberglass	[46]	960 μm	0.04[1]	–	–	–

[a] Value obtained digitalizing transmittance graphs of materials using WebPlotDigitizer tool. Wavelenghts from 0,38 to 2,5.
[b] Value obtained digitalizing transmittance graphs of materials using WebPlotDigitizer tool.

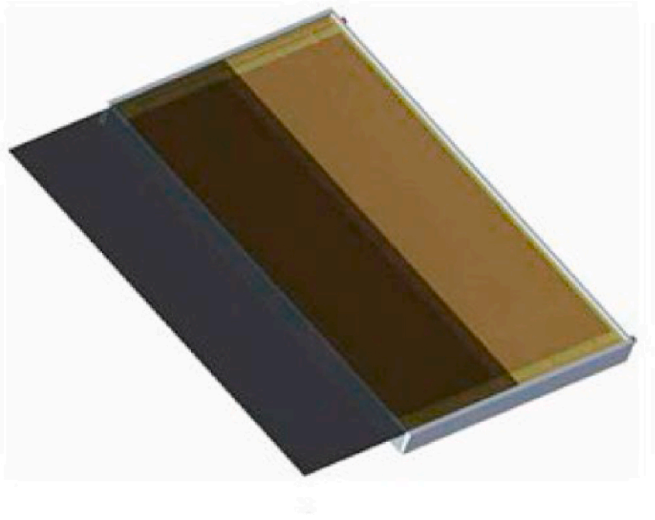

Fig. 4. Sliding adaptive cover proposed by Vall et al. [15].

generated H_2Te. The film had a relatively lower transmittance in the atmospheric windows compared to polyethylene (0.652 vs. 0.813) but also a higher decrease in transmittance in the solar range (0.047 vs. 0.891). For this reason, it is suitable to use it as a daytime radiative cooler shield.

3.1.3. Effect of aging

The continuous exposition to the atmosphere has a deteriorating effect in the optical properties of the polymers. Ali et al. [59] studied the degradation on the transparency of films of polyethylene of 50 μm under atmospheric conditions in Assiut (Egypt). The transmittance of the film dropped 41.7%, from 0.72 to 0.42 after 100 days of outdoor exposition; the radiative cooling performance decreased a 33.3%.

Carrasco et al. [73] analyzed HDPE exposed under artificial UV light with FTIR technology. Samples were prepared following the ASTM-D638 standard 0 type V. Analysis shows that the polymer undergoes chemical and structural changes that modify its mechanical properties: stiffness of HDPE increased after 120 days of exposition, Young's modulus changed from 604 MPa to 855 MPa (Fig. 7), tensile strength is reduced from 23.1 to 17.1 MPa (Fig. 7), and the strain is reduced from 231% to 7.4% (Fig. 7).

3.1.4. Effect of thickness

The thickness of the cover material has an effect on its optical properties. Ali et al. [59,60] studied the transmittances of polyethylene with different thickness, concluding that a foil of 25 μm of thickness showed better transparency than a foil of 50 μm. They verified that the decrease in the thickness of the PE foil, from 50 μm to 25 μm, supposed and increase of the performance of the radiative cooler by 8.6%.

Nwaji et al. [61] carried out a finite element analysis of the performance of a RCE system applied in five Nigerian cities. The authors modeled a flat titanium absorber coated with PET and covered with a polyethylene windscreen. Results showed that, during daytime solar collection, as the number of polyethylene windscreens increased, the circulating water temperature decreased progressively (Fig. 8).

3.1.5. Mechanical problems

Despite the favorable optical properties of polymeric covers described above, their weak mechanical properties become an inconvenient for their application outdoors: the cover has to withstand wind, tearing, rainwater [62] and snow. Dust and humidity can affect both the mechanical behavior and the optical properties of the cover [16]. Due to

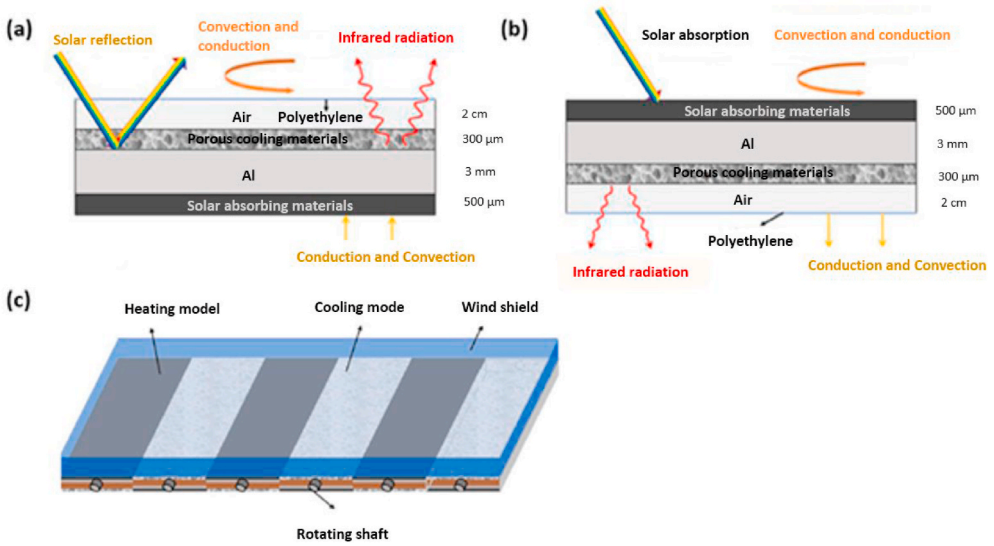

Fig. 5. Mixed radiative cooler and solar heater proposed by Liu et al. [22]. (a) Radiative cooling mode, (b) Solar heating mode and (c) rotating structure.

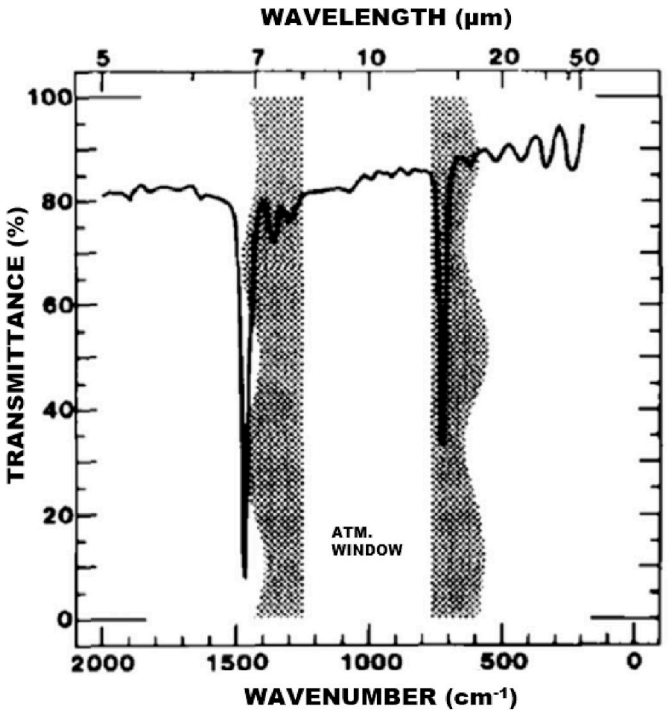

Fig. 6. Spectral transmittance of a 30 μm thick foil of HDPE [53].

its thinness, the wind can cause the fluttering of the foil. Finally, the covers are exposed to the presence of animals – birds and insects – which can damage the structure.

A new configuration for the polyethylene shape was studied by Nilsson et al. [63] in 1985. They used a screen made of three layers of corrugated polyethylene in a V-shapped arrangement (Fig. 9). When transmittance and thermal insulation was analyzed, this configuration presented a better convective performance than a flat cover, with a transmittance of 0.73. Moreover, this cover had a characteristic thickness of 4.5 cm; although it was not studied, it could add an extra structural resistance compared to flat covers.

Golaka and Exell [74] simulated a theoretical convective shield, a grid made of slats, which could deal with the previous described structural weakness. Authors performed finite elements simulations of the airflow through diverse obstacles over a radiative cooling surface: on top of the surface it was placed a grid consisting of metallic perpendicular strips (Fig. 10). The grid acts as a barrier for the airflow, reducing the total heat transferred by convective movements. A small windshield could increase the turbulence over a surface, increasing the convective heat transfer but a higher windshield avoids these problems. However, a high shield can interfere with the radiation of the surface. Authors concluded that it makes sense to use this structure where the winds produce unfavorable heat fluxes to the surface [74]. As mentioned by Gentle et al., the previous study overestimated the reduction potential of the convective heat transfer [62].

Gentle et al. proposed the use of a polymeric mesh made of UV stabilized HDPE fibers of 150 μm diameter (Fig. 11). The mesh had an effective transparency of 87% while suppressing the convection transfer

Table 4
Summary of optical properties of pigmented covers.

Pigment	Reference	Thickness	τ_{atm}	τ_{sol}	ρ_{atm}	ρ_{sol}	α_{atm}	α_{sol}
TiO_2	[65]	100 μm	0.74	0.57	–	–	–	–
TiO_2	[67]	0.12 μm	0.765	0.61	0.765	0.381	0.063	0.009
TiO_2	[67]	0.45 μm	0.731	0.412	0.731	0.581	0.115	0.007
TiO_2	[67]	0.75 μm	0.681	0.273	0.681	0.712	0.157	0.015
TiO_2	[67]	1.08 μm	0.651	0.22	0.651	0.684	0.196	0.096
TiO_2	[67]	1.82 μm	0.546	0.166	0.546	0.763	0.276	0.071
TiO_2	[67]	submicrometer	0.323	0.391	0.601	0.435	0.076	
TiO_2	[68]	100 μm	0.75	0.09		0,67		
Carbonblack	[65]	100 μm	0.74	0.24	–	–	–	–
ZnO	[68]	–	0.68	0.31		0.69		
ZnS	[68]	400 μm	0.33	0.013	0.09	0.849	0.58	0.138
ZnS	[70]	420 μm	~0.6	–	–	0.8	–	–

Table 5
Summary of optical properties of deposited films.

Film material	Reference	Thickness	τatm	τsol	ρatm	ρsol	αatm	αsol
PbSe (HC NTA)	[71]	200 μm	0.508	0.09	0.186	0.274	0.306	0.636
PbS (HC NTA)	[71]	200 μm	0.741	0.168	0.154	0.468	0.105	0.364
PbS (HC TSC)	[71]	150 μm	0.642	0.138	0.143	0.372	0.215	0.490
ZnS pigment + PbS film	[71]	–	0.488	0.162	0.331	0.35	0.629	0.629
ZnO pigment + LDPE coated with PbS film	[71]	–	0.406	0.03	0.155	0.286	0.439	0.684
MnO coated PE	[72]	50 μm	0.801	0.725	0.17	0.173	0.029	0.102
Te	[72]	0.12 μm	0.652	0.047	0.221	0.123	0.137	0.83

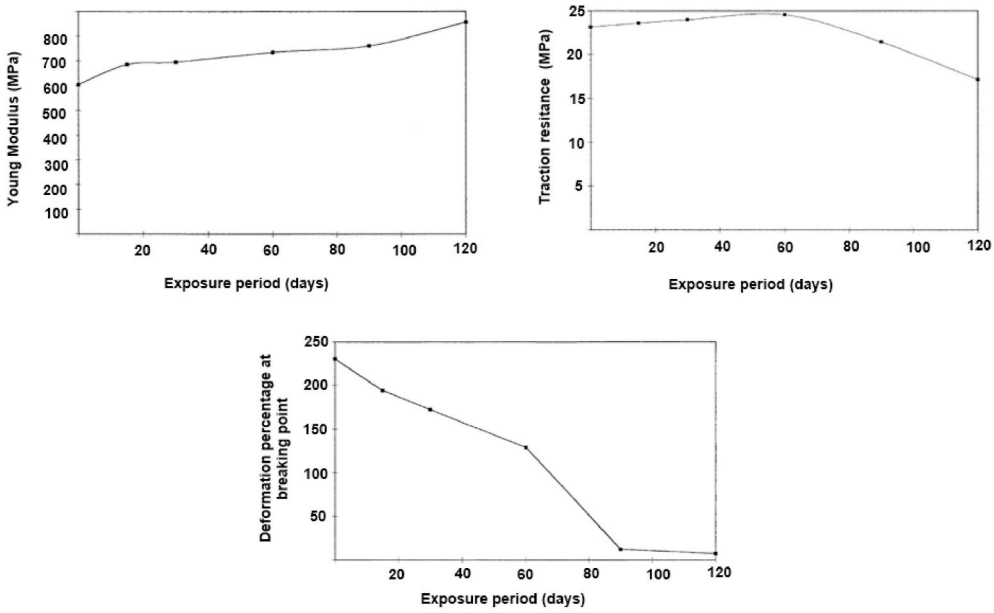

Fig. 7. Variation of Young modulus, traction resistance and strain. Modification of [73].

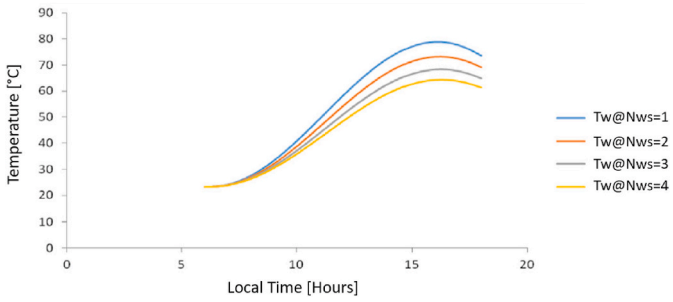

Fig. 8. Effect of number of polyethylene windscreens, under solar collection, simulated by Nwaji et al. [61].

[62]. Based on the existing use of UV stabilized mesh in the field of agriculture, authors affirmed that this configuration was expected to have a lifespan of 5 years.

3.2. Non-polymeric convective covers

3.2.1. Zinc crystals

Zinc compounds have also been investigated in the form of crystals. Compared to zinc pigments, where zinc compound constituted a small portion of the whole cover, zinc crystals are big structures constituted mainly by zinc. With the aim of obtaining a robust cover, Bathgate and Bosi [75,76] studied the thermal performance of ZnS shield. Authors compared ZnS cover with a polyethylene cover: ZnS had similar radiative cooling performances to polyethylene. Nevertheless, ZnS crystal

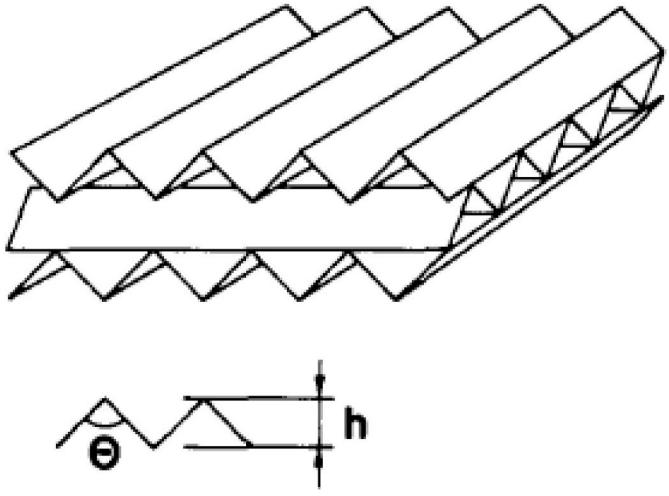

Fig. 9. Three layered corrugated foils (v-shapped) of polyethylene with high infrared transmittance and low nonradiative heat exchange [63].

covers are a durable solution. ZnS is a low toxic material, outdoor resistant and available in 4 mm thickness – 40 times thicker than PE – which provided an atmospheric window's transmittance of 64%.

Chen et al. [77] combined a highly selective emitter with a ZnSe cover to minimize solar radiation; the passive radiative cooling system was backed with a shading system which minimizes solar radiation exposition and a vacuum chamber which minimizes parasitic conductive

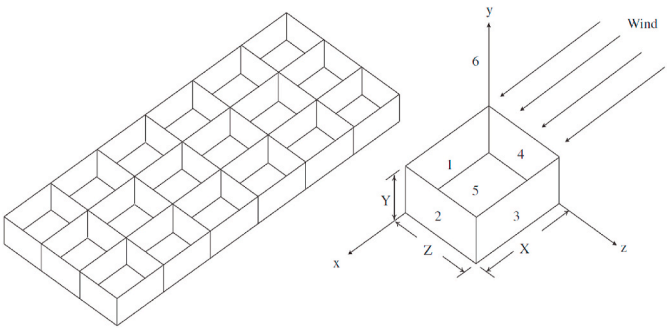

Fig. 10. Wind shield proposed by Golaka and Exell and an enlarged view of a cell unit [74].

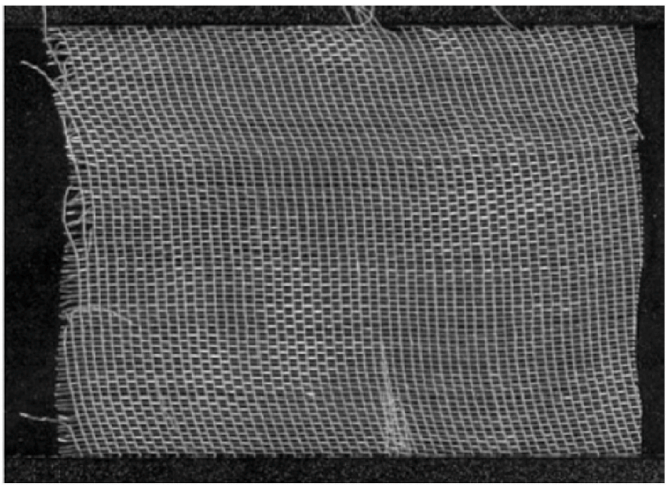

Fig. 11. Segment of the HDPE mesh [59].

and convective loses. The whole system achieved a record decrease of the surface temperature of 42 °C below ambient coinciding with the peak of solar irradiance (Fig. 12). Laatioui et al. [78] calculated the optical properties in the solar and atmospheric windows' range of the following shields: ZnS, ZnSe and ZnTe. The shields had a transmittance between 0.66 and 0.77 in the atmospheric windows and between 0.61 and 0.66 in the solar range. The transmittance was lower in the visible range (0.22–0.37).

ZnSe and ZnS crystals are materials that have a high price. Reduction of thickness and purity of the crystal would represent a reduction in cost. Nevertheless, Yashina et al. [79] described three processes of manufacturing ZnS polycrystals: chemical vapor deposition (CVD), hot pressing, and vapor deposition. The first method is based on the reaction of Zn with H_2S, while the other two processes make use of ZnS powder, which is less expensive than crystal. According to the authors, CVD is the most appealing process to fabricate ZnS crystals due to its better optical homogeneity and low impurity content [79,80].

3.2.2. *Cadmium films*

Benlattar et al. [81] studied the use of CdTe films (9.7 μm) on a 1 mm silicon substrate. The film had a relatively high reflectivity (0.38) and an elevated absorption (0.42) in the solar band and was transparent in the 8–13 μm region (0.62). One year later, in 2006, the authors presented a similar experiment, this time using a CdS sheet (1 mm). The sheet had a high transmittance in the 8–13 μm range (0.8) and a high absorptivity in the solar range (0.68) [82]. Table 6 summarizes these properties. Fig. 13 presents a visual comparison of the atmospheric window transmittance of the previous materials. It can be seen visually that polyethylene covers, CdS and zinc-based materials presented the highest transmittance.

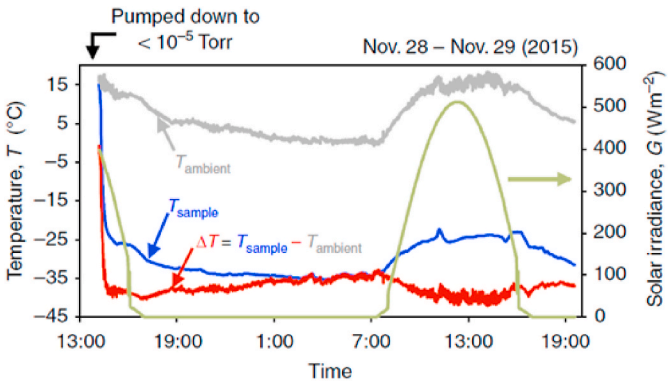

Fig. 12. Large temperature reduction below ambient through radiative cooling in a 24-h day-night cycle. A maximal cooling of 42.2 °C synchronizes with the peak of the solar irradiances [77].

4. Smart material adaptive cover

A smart material for RCE windscreen applications would switch its optical properties depending on the working mode: during daytime it should present a strong transmittance in the solar band and opacity in the infrared band; during nighttime it should be highly transparent to the infrared range. In the following sections several types of chromic materials (electrochromic, thermochromic, gasochromic and photochromic) are reviewed in order to know their suitability for RCE, as they can change their optical properties under exposure to external stimuli. These materials have been used in thermal control but, despite being widely studied in the glazing and smart window industries [83–85], the wavelength range of interest of these materials is restricted to solar range and no insights on the infrared are provided. To our knowledge, only few researches have studied the infrared range.

4.1. *Electrochromic materials*

Under the application of low magnitude voltage, electrochromic materials exhibit tunability of their optical properties [86]. These properties have been studied since the 1970s [87], mostly in the visible spectrum [88]. This technology has most of its applications in the field of smart windows [89], although they are also noteworthy in camouflage [90,91], automotive and aircraft [87,89], and thermal regulation [83].

Electrochromic materials show a battery-shaped structure (Fig. 13) consisting of five layers interspersed with transparent conductive materials, an electrolyte conducting material, an electrochromic sheet and an electron accumulation layer [92]. The working principle of this material is the redox reactions that occur when the current flows. The ions, usually Li^+ or H^+, move from the accumulation layer to the electrode, generating new energy bands in which the compound interacts with the light and, as a consequence, modifies the optical properties of the material.

Metal oxides such as WO, TiO_2, Nb_2O_5, MoO_3, NiO, IrO_2 and V_2O_5 [93] have been used as electrochromic materials to control the transmittance and emissivity properties in the visible, especially wolfram compounds being also able to act on the NIR spectrum [94].

Mandal et al. [95] studied the existing change in the infrared spectrum of a lithium-titanium-oxygen material. In the $Li_4Ti_5O_{12}$ form it exhibits low visible and long-infrared absorbance; in the $Li_7Ti_5O_{12}$ form it has high emission throughout the IR, thus allowing thermal regulation. According to the authors, this material may have application as radiative surfaces for radiative cooling and solar heating devices. Franke et al. [96] studied the optical properties of electrochromic surfaces based on wolfram and achieved a modulation of their emissivity. Xu

Table 6
Summary of optical properties of non-polymeric covers.

Cover material	Reference	Thickness	τ_{atm}	τ_{sol}	ρ_{atm}	ρ_{sol}	α_{atm}	α_{sol}
ZnS	[75]	4 mm	0.64	–	–	–	–	–
ZnS	[76]	4 mm	0.64	–	–	–	–	–
ZnS	[78]	1 mm	0.77	0.66	0.12	0.21	0.11	0.13
ZnSe	[76]	7.1 mm	0.7	–	–	–	–	–
ZnSe	[77]	–	0.87	–	–	–	–	–
ZnSe	[78]	1 mm	0.71	0.65	0.17	0.20	0.12	0.15
ZnTe	[78]	1 mm	0.66	0.61	0.21	0.22	0.13	0.17
Tefzel	[76]	200 μm	0.1	–	–	–	–	–
Silicon	[76]	0.6 mm	0.47	–	–	–	–	–
CdTe film + Si substrate	[81]	9.7 μm + 1 mm	0.58	0.3	0.3	0.38	0.42	0.22
CdTe film + Si substrate	[81]	9.7 μm + 1 mm	0.62	0.28	0.01	0.07	0.37	0.71
CdS film	[82]	1 mm	0.8	0.3	0.01	0.02	0.19	0.68

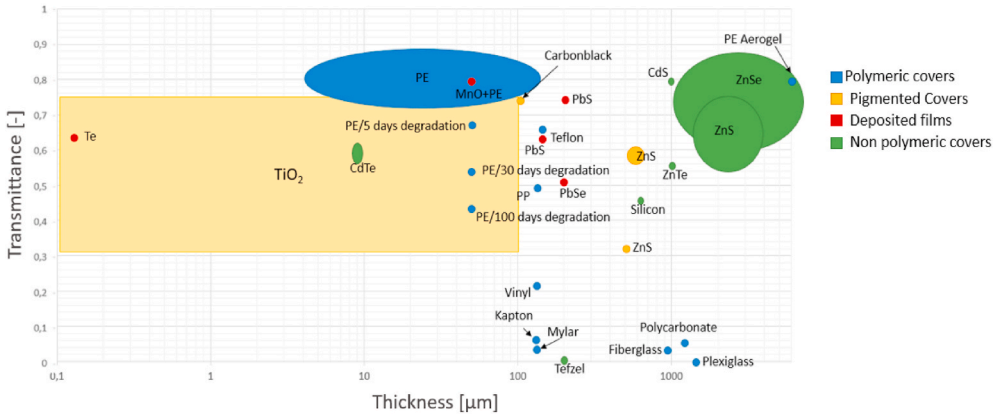

Fig. 13. Comparison of experimental transmittances in the atmospheric window of different materials grouped in: polymeric, deposited films, pigmented covers and non-polymeric materials.

et al. [97] achieved changes of 0.4 of emissivity in the 8–14 μm range -atmospheric window-in a device based on H_2SO_4-doped polyaniline films, allowing radiative cooling under low voltage.

4.2. Thermochromic materials

Thermochromic materials respond to temperature changes by modifying their optical properties [93]. Thermochromic materials maintain a highly emissive or transmitting semiconductor structure in the infrared; when the transition point (T_c) is reached, the material behaves like a semi metal, with high reflectivity in the infrared band [98]. These materials find their applications in the fields of energy saving, thermal control and camouflage [99] and glazing [100].

Vanadium dioxide (VO_2) is a phase change material usually studied in thermochromic applications. At a temperature below 68 °C, vanadium dioxide presents high emissivity in the IR, whereas when the temperature is above the transition point, it is highly reflective to IR wavelengths. According to Liu et al. [98], a 900 nm VO_2 thin film exhibited 0.8–0.9 emittance in the IR below transition conditions whereas for above conditions the emittance fell between 0.2 and 0.3. In comparison, thicker films of vanadium dioxide offer better thermochromic properties between modes than thin films.

Doping vanadium dioxide the transition temperature can be controlled. When doped with wolfram transition temperature can be reduced to 30 °C [101]. Other authors have doped vanadium dioxide with terbium cation (Tb^{3+}). Although an improvement in transmittance was shown, the transition temperature reduction was much lower (from 67.5 °C to 60 °C) [102]. Alternatively, Chen et al. [103] reduced transition temperature to 35 °C with an undoped VO_2 multilayered structure.

Thermochromic material, such as vanadium dioxide, can be used as switchers to control the effective emissivity surfaces in order to achieve a turning "on-off" radiative cooler [104]. Metamaterial configurations of thermochromic materials enhance radiative cooling properties [105]. Sun et al. [106] demonstrated that, at room temperature, an VO_2 metamaterial emitter radiated in 3–5 μm and 8–14 μm range; at high temperature strong radiation was gathered in the 5–8 μm range. Tazawa et al. [107,108] estimated a maximum cooling power of near 50 W/m^2 for a vanadium-doped surface. Ono et al. [109] simulated the performance of a VO_2 metamaterial based radiative cooler which initiated when ambient temperature was above a transition point; the results showed a maximum cooling power peak of 120 W/m^2 (Fig. 14). Kort-Kamp et al. [110] also simulated the performance of a photonic VO_2 radiator; the results showed that a 6 °C reduction from the ambient could be achieved under ~100 W/m^2 cooling rates (see Fig. 15).

Polymer can also exhibit thermochromism [111]. La et al. [112] studied a polyampolyte hydrogel which showed a high contrast of 80% in the visible band: from opaque at low temperature to transparent at high temperature. The transmittance in the mid-infrared and long-infrared was lower in both cases.

4.3. Gasochromic materials and gas slab

Gasochromic materials exhibit a change in coloration of films based on wolfram due to the presence of hydrogen [88,113]. These materials have favorable points over electrochromic and thermochromic material: gasochromic are cheaper and simpler and allow better modulation of the transmittance, being able to achieve intermediate transmittances [100]. Gasochromic smart windows' switching properties can decrease the annual thermal HVAC consumptions by 25%–35% [85]. Nevertheless, they may still not have an application in radiative cooling or solar heating fields, as the infrared range has not been studied.

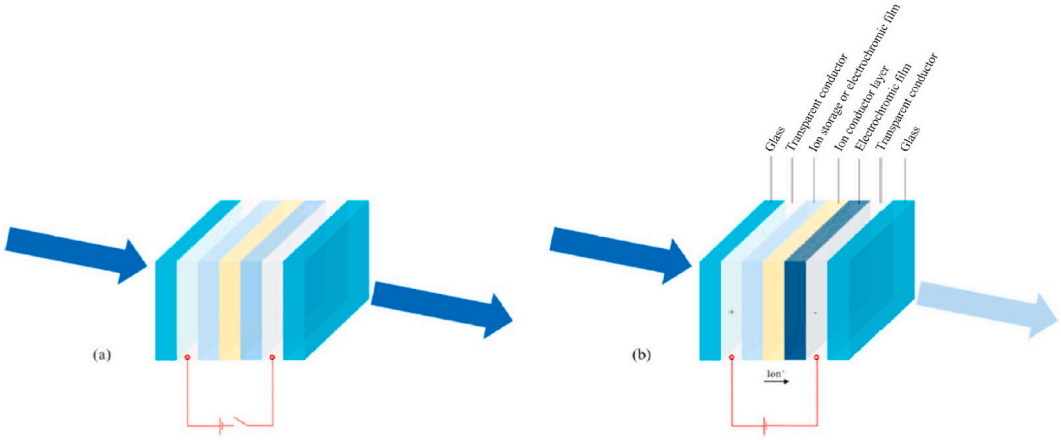

Fig. 14. Illustration of an electrochromic window bleached (a) and colored (b) [92].

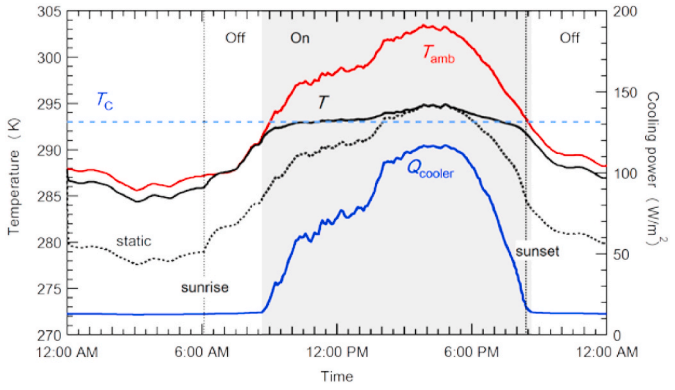

Fig. 15. Thermal performance of a VO_2 metamaterial based radiative cooler (black curve) over a 24h cycle. Blue curve represents the cooling power of the radiative cooler [109]. (For interpretation of the references to color in this figure legend, the reader is referred to the Web version of this article.)

Radiative cooling has been tested with selectively emitting infrared gases confined in the air gap between the emitting/absorbing surface and the infrared transparent convective cover [114]. However, little research has been conducted. Spectrometry techniques found that ethylene (C_2H_4), ethyl oxide (C_2H_4O) and ammonia (NH_3) [115–117] are three gases which –in the presence of low humidity– show high emissivity in the atmospheric window wavelengths (8–14 μm). In an experiment with ethylene gas, under daytime conditions, authors measured a drop of 10 °C with respect to the environment [117].

4.4. Photochromic materials

Under exposure to ultraviolet light photochromic materials turn dark [28]. This photochromic switching is a fast and reversible process [88]. To our knowledge, photochromic materials do not present yet applications in the radiative cooling field.

Photochromism occurs when a transition in a molecule, such as azobenzene, spiropyran, furylfulgide, and diarylethene [93], between two isomers with different optical properties exists [118]. Other metal oxides –MoO_3, WO_3, V_2O_5, Nb_2O_5, ZnO, and TiO_2 [93]– also exhibit photochromism.

5. Conclusions

In this study the concept of RCE has been presented. Covers, or windscreens, with switching optical properties placed on top of absorber/emitter surface can be used in order to achieve mixed solar heating and radiative cooling.

This paper has also discussed the influence of convection phenomena on radiative cooling and solar heating surfaces and the different approaches used by various authors to calculate this contribution as a direct function of wind speed. In order to achieve subambient temperatures through radiative cooling, the need to reduce these negative gains through windscreens or convective shields has been emphasized. Then, adaptive windscreens in RCE devices allow the switching between working modes and a reduction of thermal exchanges, enhancing the performance.

Windscreens can be found in many of experimental research in the fields of radiative cooling and RCE analyzed in this paper. However, they are presented as an additional complement, meaning that the effects of using a windscreen are, in general, not examined.

The article reviewed and classified the different types of adaptive covers used in order to reduce convective gains/losses, for later use in mixed applications of both radiative cooling and solar heating. These mixed applications have been classified into two major groups depending on whether they rely on a single smart material or a combination of different materials (exchangeable covers). Polyethylene is the most widely used material in radiative cooling and RCE applications due to its high transmittance in the 8–14 μm band, the main atmospheric window. Different prototypes have been developed that allow both night radiation and daytime collection and the ability of these devices to meet the demands of thermal loads has also been modeled. Polyethylene presents serious structural and aging disadvantages. Increasing the thickness of the material is not considered an optimal solution as it worsens the total transmittance. Pigmented covers block a big portion of the sunlight and are not appropriate for RCE applications. Alternatively, zinc crystals offer some transmittance in the solar range and could be used as thick windscreen in RCE applications. However, they are an expensive solution.

Finally, authors suggest that chromic materials could become a durable solution for windscreen in radiative cooling-solar heating applications. These materials are of high interest in smart windows and glazing technologies. Due to this fact, papers analyzed do not present information of the performance in the infrared region. On the other hand, the chromic materials already studied in radiative cooling applications have been used as emitters so these materials have no seemingly useful properties as windscreen. After this review, authors propose the characterization of the optical properties, in both the solar range and the atmospheric windows' range, of chromic materials as the next research step on the path of improving the performance of combined solar heating and radiative cooling applications.

CRediT authorship contribution statement

Roger Vilà: Conceptualization, Investigation, Data curation, Visualization, Writing – original draft. **Ingrid Martorell:** Conceptualization, Investigation, Writing – review & editing. **Marc Medrano:** Conceptualization, Investigation, Writing – review & editing, Supervision. **Albert Castell:** Conceptualization, Writing – review & editing, Supervision, Project administration, Funding acquisition.

Declaration of competing interest

The authors declare that they have no known competing financial interests or personal relationships that could have appeared to influence the work reported in this paper.

Acknowledgements

The work was partially funded by the Catalan Government under grant agreement (2017 SGR 659), and the Spanish government under grant agreement RTI2018-097669-A-I00 (Ministerio de Ciencia, Innovación y Universidades).

References

[1] IEA, "Global energy demand rose by 2.3% in 2018, its fastest pace in the last decade," IEA, Mar. 26, accessed Jan. 23, 2020, https://www.iea.org/news/global-energy-demand-rose-by-23-in-2018-its-fastest-pace-in-the-last-decade, 2019.
[2] J. Cook, et al., Consensus on consensus: a synthesis of consensus estimates on human-caused global warming, Environ. Res. Lett. 11 (4) (Apr. 2016), 048002, https://doi.org/10.1088/1748-9326/11/4/048002.
[3] Directive 2009/28/EC of the European Parliament and of the Council of 23 April 2009 on the Promotion of the Use of Energy from Renewable Sources and Amending and Subsequently Repealing Directives 2001/77/EC and 2003/30/EC, Jun. 2009, https://doi.org/10.1007/978-1-137-54507-7_21.
[4] Directive (EU), Of the European Parliament and of the Council of 30 May 2018 Amending Directive 2010/31/EU on the Energy Performance of Buildings and Directive 2012/27, EU on energy efficiency, 2018, p. 17.
[5] Commission recommendatoin (EU), on Building Renovation - (Notified under Document C(2019) 3352), 786 - of 8 May 2019, 2019, p. 46.
[6] Project Europe 2030: Challenges and Opportunities : a Report to the European Council by the Reflection Group on the Future of the EU 2030, Publications Office of the European Union, Luxemburg, 2010.
[7] European Comission, Energy performance of buildings directive. https://ec.europa.eu/energy/en/topics/energy-efficiency/energy-performance-of-buildings/energy-performance-buildings-directive#documents, 2018 accessed Jan. 23,.
[8] Eurostat, Energy Consumption in Households, May 2019. https://ec.europa.eu/eurostat/statistics-explained/index.php?title=Energy_consumption_in_households#Use_of_energy_products_in_households_by_purpose.
[9] M. Santamouris, J. Feng, Recent progress in daytime radiative cooling: is it the air conditioner of the future? Buildings 8 (12) (Dec. 2018) 168, https://doi.org/10.3390/buildings8120168.
[10] S.Y. Jeong, C.Y. Tso, M. Zouagui, Y.M. Wong, C.Y.H. Chao, A numerical study of daytime passive radiative coolers for space cooling in buildings, Build. Simul. 11 (5) (Oct. 2018) 1011–1028, https://doi.org/10.1007/s12273-018-0474-4.
[11] E. Rephaeli, A. Raman, S. Fan, Ultrabroadband photonic structures to achieve high-performance daytime radiative cooling, Nano Lett. 13 (4) (Apr. 2013) 1457–1461, https://doi.org/10.1021/nl4004283.
[12] B. Ko, D. Lee, T. Badloe, J. Rho, Metamaterial-based radiative cooling: towards energy-free all-day cooling, Energies 12 (1) (Dec. 2018) 89, https://doi.org/10.3390/en12010089.
[13] M.M. Hossain, B. Jia, M. Gu, A metamaterial emitter for highly efficient radiative cooling, Adv. Opt. Mater. 3 (8) (Aug. 2015) 1047–1051, https://doi.org/10.1002/adom.201500119.
[14] P. Berdahl, R. Fromberg, The thermal radiance of clear skies, Sol. Energy 29 (4) (1982) 299–314, https://doi.org/10.1016/0038-092X(82)90245-6.
[15] S. Vall, A. Castell, M. Medrano, Energy savings potential of a novel radiative cooling and solar thermal collection concept in buildings for various world climates, Energy Technol. 6 (11) (Nov. 2018) 2200–2209, https://doi.org/10.1002/ente.201800164.
[16] T.E. Johnson, Radiation cooling of structures with infrared transparent wind screens, Sol. Energy 17 (3) (1975) 173–178, https://doi.org/10.1016/0038-092X(75)90056-0.
[17] A.P. Raman, M.A. Anoma, L. Zhu, E. Rephaeli, S. Fan, Passive radiative cooling below ambient air temperature under direct sunlight, Nature 515 (7528) (Nov. 2014) 540–544, https://doi.org/10.1038/nature13883.
[18] D. Zhao, et al., Subambient cooling of water: toward real-world applications of daytime radiative cooling, Joule 3 (1) (Jan. 2019) 111–123, https://doi.org/10.1016/j.joule.2018.10.006.
[19] M. Matsuta, S. Terada, H. Ito, Solar Heating and radiative cooling using a solar collector-sky radiator with a spectrally selective surface, Sol. Energy 39 (3) (1987) 183–186.
[20] M. Hu, G. Pei, Q. Wang, J. Li, Y. Wang, J. Ji, Field test and preliminary analysis of a combined diurnal solar heating and nocturnal radiative cooling system, Appl. Energy 179 (2016) 899–908, https://doi.org/10.1016/j.apenergy.2016.07.066.
[21] L. Long, Y. Yang, L. Wang, Simultaneously enhanced solar absorption and radiative cooling with thin silica micro-grating coatings for silicon solar cells, Sol. Energy Mater. Sol. Cells 197 (Aug. 2019) 19–24, https://doi.org/10.1016/j.solmat.2019.04.006.
[22] J. Liu, et al., Research on the performance of radiative cooling and solar heating coupling module to direct control indoor temperature, Energy Convers. Manag. 205 (Feb. 2020) 112395, https://doi.org/10.1016/j.enconman.2019.112395.
[23] S. Vall, M. Medrano, C. Solé, A. Castell, Combined radiative cooling and solar thermal collection: experimental proof of concept, Energies 13 (4) (Feb. 2020) 893, https://doi.org/10.3390/en13040893.
[24] X. Lu, P. Xu, H. Wang, T. Yang, J. Hou, Cooling potential and applications prospects of passive radiative cooling in buildings: the current state-of-the-art, Renew. Sustain. Energy Rev. 65 (Nov. 2016) 1079–1097, https://doi.org/10.1016/j.rser.2016.07.058.
[25] S. Vall, A. Castell, Radiative cooling as low-grade energy source: a literature review, Renew. Sustain. Energy Rev. 77 (Sep. 2017) 803–820, https://doi.org/10.1016/j.rser.2017.04.010.
[26] G.N. Nwaji, C.A. Okoronkwo, N.V. Ogueke, E.E. Anyanwu, Hybrid solar water heating/nocturnal radiation cooling system I: a review of the progress, prospects and challenges, Energy Build. 198 (Sep. 2019) 412–430, https://doi.org/10.1016/j.enbuild.2019.06.017.
[27] D. Zhao, et al., Radiative sky cooling: fundamental principles, materials, and applications, Appl. Phys. Rev. 6 (Jun. 2019), 021306, https://doi.org/10.1063/1.5087281.
[28] C.G. Granqvist, G.A. Niklasson, Solar energy materials for thermal applications: a primer, Sol. Energy Mater. Sol. Cells 180 (Jun. 2018) 213–226, https://doi.org/10.1016/j.solmat.2018.02.004.
[29] S. Buddhiraju, P. Santhanam, S. Fan, Thermodynamic limits of energy harvesting from outgoing thermal radiation, Proc. Natl. Acad. Sci. Unit. States Am. 115 (16) (Apr. 2018) E3609–E3615, https://doi.org/10.1073/pnas.1717595115.
[30] R. Zevenhoven, M. Fält, Radiative cooling through the atmospheric window: a third, less intrusive geoengineering approach, Energy 152 (Jun. 2018) 27–33, https://doi.org/10.1016/j.energy.2018.03.084.
[31] M.G. Meir, J.B. Rekstad, O.M. LØvvik, A study of a polymer-based radiative cooling system, Sol. Energy 73 (6) (Dec. 2002) 403–417, https://doi.org/10.1016/S0038-092X(03)00019-7.
[32] M. Zeyghami, D.Y. Goswami, E. Stefanakos, A review of clear sky radiative cooling developments and applications in renewable power systems and passive building cooling, Sol. Energy Mater. Sol. Cells 178 (May 2018) 115–128, https://doi.org/10.1016/j.solmat.2018.01.015.
[33] Y. Cui, Y. Wang, Q. Huang, S. Wei, Effect of radiation and convection heat transfer on cooling performance of radiative panel, Renew. Energy 99 (Dec. 2016) 10–17, https://doi.org/10.1016/j.renene.2016.06.025.
[34] J.A. Duffie, W.A. Beckman, Solar Engineering of Thermal Processes, John Wiley & Sons, Inc., Hoboken, NJ, USA, 2013, https://doi.org/10.1002/9781118671603.
[35] J. Li, et al., Experimental study on a novel photovoltaic thermal system using amorphous silicon cells deposited on stainless steel, Energy 159 (Sep. 2018) 786–798, https://doi.org/10.1016/j.energy.2018.06.127.
[36] E. Erell, D. Pearlmutter, T. Williamson, Urban Microclimate: Designing the Spaces between Buildings, Routledge, 2012.
[37] K.W. Böer, J.A. Duffie, Advances in Solar Energy: an Annual Review of Research and Development, Springer Science & Business Media, 2012.
[38] E. Sartori, Convection coefficient equations for forced air flow over flat surfaces, Sol. Energy 80 (9) (Sep. 2006) 1063–1071, https://doi.org/10.1016/j.solener.2005.11.001.
[39] S. Sharples and P. S. Charlesworth, "Full Scale Measurements of Wind Induced Convective Heat Transfer from a Roof Mounted Flat-Plate Solar Collector," p. 9.
[40] B. Givoni, Passive Low Energy Cooling of Buildings. John Wiley & Sons.
[41] G. Mihalakakou, A. Ferrante, J.O. Lewis, The cooling potential of a metallic nocturnal radiator, Energy Build. 28 (3) (Nov. 1998) 251–256, https://doi.org/10.1016/S0378-7788(98)00006-1.
[42] Y. Choi, M. Mae, H. Bae Kim, Thermal performance improvement method for air-based solar heating systems, Sol. Energy 186 (Jul. 2019) 277–290, https://doi.org/10.1016/j.solener.2019.04.061.
[43] S. Furbo, L. Jivan Shah, Thermal advantages for solar heating systems with a glass cover with antireflection surfaces, Sol. Energy 74 (6) (Jun. 2003) 513–523, https://doi.org/10.1016/S0038-092X(03)00186-5.
[44] B. Orel, M. Klanjsek Gunde, A. Krainer, Radiative cooling efficiency of white pigmented paints, Sol. Energy 50 (6) (1993) 477–482.
[45] B. Bartoli, S. Catalanotti, B. Coluzzi, V. Cuomo, V. Silvestrini, G. Troise, Nocturnal and diurnal performances of selective radiators, Appl. Energy 3 (4) (1977) 267–286, https://doi.org/10.1016/0306-2619(77)90015-0.
[46] P.T. Tsilingiris, Comparative evaluation of the infrared transmission of polymer films, Energy Convers. Manag. 44 (18) (Nov. 2003) 2839–2856, https://doi.org/10.1016/S0196-8904(03)00066-9.

[47] A. Leroy, et al., High-performance subambient radiative cooling enabled by optically selective and thermally insulating polyethylene aerogel, Sci. Adv. 5 (10) (Oct. 2019), eaat9480, https://doi.org/10.1126/sciadv.aat9480.

[48] Z. Xu, et al., A new crystal Mg11(HPO3)8(OH)6 for daytime radiative cooling, Sol. Energy Mater. Sol. Cells 185 (Oct. 2018) 536–541, https://doi.org/10.1016/j.solmat.2018.06.012.

[49] Y. Fu, J. Yang, Y.S. Su, W. Du, Y.G. Ma, Daytime passive radiative cooler using porous alumina, Sol. Energy Mater. Sol. Cells 191 (Mar. 2019) 50–54, https://doi.org/10.1016/j.solmat.2018.10.027.

[50] M. Hu, B. Zhao, X. Ao, Y. Su, G. Pei, Numerical study and experimental validation of a combined diurnal solar heating and nocturnal radiative cooling collector, Appl. Therm. Eng. 145 (Dec. 2018) 1–13, https://doi.org/10.1016/j.applthermaleng.2018.08.097.

[51] M. Hu, et al., Experimental study on a hybrid photo-thermal and radiative cooling collector using black acrylic paint as the panel coating, Renew. Energy 139 (Aug. 2019) 1217–1226, https://doi.org/10.1016/j.renene.2019.03.013.

[52] M.A. Al-Nimr, Z. Kodah, B. Nassar, A theoretical and experimental investigation of a radiative cooling system, Sol. Energy 63 (6) (Dec. 1998) 367–373, https://doi.org/10.1016/S0038-092X(98)00098-X.

[53] B. Zhao, M. Hu, X. Ao, X. Huang, X. Ren, G. Pei, Conventional photovoltaic panel for nocturnal radiative cooling and preliminary performance analysis, Energy 175 (May 2019) 677–686, https://doi.org/10.1016/j.energy.2019.03.106.

[54] M. Hu, B. Zhao, J. li, Y. Wang, G. Pei, Preliminary Thermal Analysis of a Combined Photovoltaic-Photothermic-Nocturnal Radiative Cooling System, " *Energy*, Jan. 2016, https://doi.org/10.1016/j.energy.2017.03.075.

[55] M. Hu, G. Pei, L. Li, R. Zheng, J. Li, J. Ji, Theoretical and experimental study of spectral selectivity surface for both solar heating and radiative cooling, Int. J. Photoenergy 2015 (2015) 1–9, https://doi.org/10.1155/2015/807875.

[56] M. Hu, et al., Feasibility research on a double-covered hybrid photo-thermal and radiative sky cooling module, Sol. Energy 197 (Feb. 2020) 332–343, https://doi.org/10.1016/j.solener.2020.01.022.

[57] X. Ao, M. Hu, B. Zhao, N. Chen, G. Pei, C. Zou, Preliminary experimental study of a specular and a diffuse surface for daytime radiative cooling, Sol. Energy Mater. Sol. Cells 191 (Mar. 2019) 290–296, https://doi.org/10.1016/j.solmat.2018.11.032.

[58] C. Liu, Y. Wu, B. Wang, C.Y. Zhao, H. Bao, Effect of atmospheric water vapor on radiative cooling performance of different surfaces, Sol. Energy 183 (May 2019) 218–225, https://doi.org/10.1016/j.solener.2019.03.011.

[59] A.H.H. Ali, H. Saito, I.M.S. Taha, K. Kishinami, I.M. Ismail, Effect of aging, thickness and color on both the radiative properties of polyethylene films and performance of the nocturnal cooling unit, Energy Convers. Manag. 39 (1–2) (Jan. 1998) 87–93, https://doi.org/10.1016/S0196-8904(96)00174-4.

[60] A. Hamza H. Ali, I.M.S. Taha, I.M. Ismail, Cooling of water flowing through a night sky radiator, Sol. Energy 55 (4) (1995) 235–253, https://doi.org/10.1016/0038-092X(95)00030-U.

[61] G.N. Nwaji, C.A. Okoronkwo, N.V. Ogueke, E.E. Anyanwu, Investigation of a hybrid solar collector/nocturnal radiator for water heating/cooling in selected Nigerian cities, Renew. Energy 145 (Jan. 2020) 2561–2574, https://doi.org/10.1016/j.renene.2019.07.144.

[62] A.R. Gentle, K.L. Dybdal, G.B. Smith, Polymeric mesh for durable infra-red transparent convection shields: applications in cool roofs and sky cooling, Sol. Energy Mater. Sol. Cells 115 (Aug. 2013) 79–85, https://doi.org/10.1016/j.solmat.2013.03.001.

[63] N.A. Nilsson, T.S. Eriksson, C.G. Granqvist, Infrared-transparent convection shields for radiative cooling: initial results on corrugated polyethylene foils, Sol. Energy Mater. 12 (5) (1985) 327–333, https://doi.org/10.1016/0165-1633(85)90002-4.

[64] B. Bhatia, et al., Passive directional sub-ambient daytime radiative cooling, Nat. Commun. 9 (1) (2018) 5001, https://doi.org/10.1038/s41467-018-07293-9. Nov.

[65] A. Andretta, B. Bartoli, B. Coluzzi, V. Cuomo, Selective surfaces for natural cooling devices, J. Phys. Colloq. 42 (C1) (Jan. 1981) C1-423–C1-430, https://doi.org/10.1051/jphyscol:1981131.

[66] G. A. Niklasson and T. S. Eriksson, "Radiative Cooling with Pigmented Polyethylene Foils".

[67] Y. Mastai, Y. Diamant, S.T. Aruna, A. Zaban, TiO2 nanocrystalline pigmented polyethylene foils for radiative cooling applications: synthesis and characterization, Langmuir 17 (22) (2001) 7118–7123.

[68] T.M.J. Nilsson, G.A. Niklasson, Radiative cooling during the day: simulations and experiments on pigmented polyethylene cover foils, Sol. Energy Mater. Sol. Cells 37 (1) (Apr. 1995) 93–118, https://doi.org/10.1016/0927-0248(94)00200-2.

[69] T.M. Nilsson, W.E. Vargas, G.A. Niklasson, "Pigmented Foils for Radiative Cooling and Condensation Irrigation," Freiburg, Federal Republic of Germany, Sep. 1994, pp. 193–204, https://doi.org/10.1117/12.185370.

[70] T.M.J. Nilsson, G.A. Niklasson, C.G. Granqvist, A solar reflecting material for radiative cooling applications: ZnS pigmented polyethylene, Sol. Energy Mater. Sol. Cells 28 (2) (1992) 175–193, https://doi.org/10.1016/0927-0248(92)90010-M.

[71] K.D. Dobson, G. Hodes, Y. Mastai, Thin semiconductor films for radiative cooling applications, Sol. Energy Mater. Sol. Cells 80 (3) (2003) 283–296, https://doi.org/10.1016/j.solmat.2003.06.007.

[72] T. Engelhard, E.D. Jones, I. Viney, Y. Mastai, G. Hodes, "Deposition of tellurium films by decomposition of electrochemically- generated H 2 Te : application to radiative cooling devices 370 (2000) 101–105.

[73] F. Carrasco, P. Pag, Artificial aging of high-density polyethylene by ultraviolet irradiation, Eur. Polym. J. 8 (2001).

[74] A. Golaka, R.H.B. Exell, An investigation into the use of a wind shield to reduce the convective heat flux to a nocturnal radiative cooling surface, Renew. Energy 32 (4) (Apr. 2007) 593–608, https://doi.org/10.1016/j.renene.2006.03.007.

[75] S.G. Bosi, S.N. Bathgate, D.R. Mills, At last! A durable convection cover for atmospheric window radiative cooling applications 57 (2014) 1997–2004, https://doi.org/10.1016/j.egypro.2014.10.064.

[76] S.N. Bathgate, S.G. Bosi, A robust convection cover material for selective radiative cooling applications, Sol. Energy Mater. Sol. Cells 95 (10) (Oct. 2011) 2778–2785, https://doi.org/10.1016/j.solmat.2011.05.027.

[77] Z. Chen, L. Zhu, A. Raman, S. Fan, "Radiative cooling to deep sub-freezing temperatures through a 24-h day–night cycle, Nat. Commun. 7 (2016) 13729, https://doi.org/10.1038/ncomms13729. Dec.

[78] S. Laatioui, M. Benlattar, M. Mazroui, K. Saadouni, Zinc monochalcogenide thin films ZnX (X = S, Se, Te) as radiative cooling materials, Optik 166 (Aug. 2018) 24–30, https://doi.org/10.1016/j.ijleo.2018.04.004.

[79] E.V. Yashina, Preparation and properties of polycrystalline ZnS for IR applications 39 (7) (2003) 6.

[80] P. Biswas, P. Ramavath, R. Johnson, K.V. Ravi, Fabrication of IR transparent zinc sulphide plate by chemical vapour deposition (CVD), Indian J. Chem. Technol. 5 (2016).

[81] M. Benlattar, E.M. Oualim, M. Harmouchi, A. Mouhsen, A. Belafhal, Radiative properties of cadmium telluride thin film as radiative cooling materials, Opt Commun. 256 (1–3) (2005) 10–15, https://doi.org/10.1016/j.optcom.2005.06.033.

[82] M. Benlattar, E.M. Oualim, T. Mouhib, M. Harmouchi, A. Mouhsen, A. Belafhal, Thin cadmium sulphide film for radiative cooling application, Opt Commun. 267 (1) (Nov. 2006) 65–68, https://doi.org/10.1016/j.optcom.2006.06.050.

[83] L. Giovannini, F. Favoino, V. Serra, M. Zinzi, Thermo-chromic glazing in buildings: a novel methodological framework for a multi-objective performance evaluation, Energy Procedia 158 (Feb. 2019) 4115–4122, https://doi.org/10.1016/j.egypro.2019.01.822.

[84] J. Hoon Lee, J. Jeong, Y. Tae Chae, Optimal control parameter for electrochromic glazing operation in commercial buildings under different climatic conditions, Appl. Energy 260 (Feb. 2020) 114338, https://doi.org/10.1016/j.apenergy.2019.114338.

[85] W. Feng, L. Zou, G. Gao, G. Wu, J. Shen, W. Li, Gasochromic smart window: optical and thermal properties, energy simulation and feasibility analysis, Sol. Energy Mater. Sol. Cells 144 (Jan. 2016) 316–323, https://doi.org/10.1016/j.solmat.2015.09.029.

[86] C.M. Lampert, Innovative solar optical materials, Opt. Eng. 23 (1) (Feb. 1984), https://doi.org/10.1117/12.7973260.

[87] G.A. Niklasson, C.G. Granqvist, Electrochromics for smart windows: thin films of tungsten oxide and nickel oxide, and devices based on these, J. Mater. Chem. 17 (2) (2007) 127–156, https://doi.org/10.1039/B612174H.

[88] C.M. Lampert, Chromogenic smart materials, Mater. Today 7 (3) (Mar. 2004) 28–35, https://doi.org/10.1016/S1369-7021(04)00123-3.

[89] G. Gorgolis, D. Karamanis, Solar energy materials for glazing technologies, Sol. Energy Mater. Sol. Cells 144 (Jan. 2016) 559–578, https://doi.org/10.1016/j.solmat.2015.09.040.

[90] H. Yu, et al., A feasible strategy for the fabrication of camouflage electrochromic fabric and unconventional devices, Electrochem. Commun. 102 (May 2019) 31–36, https://doi.org/10.1016/j.elecom.2019.03.006.

[91] L. Zhang, Q. Zhang, H. Ye, Design of infrared camouflage cloak for underground silos, Def. Technol. (Nov. 2019), https://doi.org/10.1016/j.dt.2019.11.001. S2214914719308177.

[92] S.D. Rezaei, S. Shannigrahi, S. Ramakrishna, A review of conventional, advanced, and smart glazing technologies and materials for improving indoor environment, Sol. Energy Mater. Sol. Cells 159 (Jan. 2017) 26–51, https://doi.org/10.1016/j.solmat.2016.08.026.

[93] Y. Wang, E.L. Runnerstrom, D.J. Milliron, Switchable materials for smart windows, Annu. Rev. Chem. Biomol. Eng. 7 (1) (Jun. 2016) 283–304, https://doi.org/10.1146/annurev-chembioeng-080615-034647.

[94] C. Guo, S. Yin, M. Yan, T. Sato, Facile synthesis of homogeneous CsxWO3 nanorods with excellent low-emissivity and NIR shielding property by a water controlled-release process, J. Mater. Chem. 21 (13) (2011) 5099, https://doi.org/10.1039/c0jm04379f.

[95] J. Mandal, S. Du, M. Dontigny, K. Zaghib, N. Yu, Y. Yang, "Li $_4$ Ti $_5$ O $_{12}$: a visible-to-infrared broadband electrochromic material for optical and thermal management, Adv. Funct. Mater. 28 (36) (Sep. 2018) 1802180, https://doi.org/10.1002/adfm.201802180.

[96] E.B. Franke, C.L. Trimble, J.S. Hale, M. Schubert, J.A. Woollam, Infrared switching electrochromic devices based on tungsten oxide, J. Appl. Phys. 88 (10) (Nov. 2000) 5777–5784, https://doi.org/10.1063/1.1319325.

[97] G. Xu, et al., A visible-to-infrared broadband flexible electrochromic device based polyaniline for simultaneously variable optical and thermal management, Sol. Energy Mater. Sol. Cells 208 (May 2020) 110356, https://doi.org/10.1016/j.solmat.2019.110356.

[98] D. Liu, H. Cheng, W. Zheng, C. Zhang, Infrared thermochromic properties of VO2 thin films prepared through aqueous sol-gel process, J. Wuhan Univ. Technol.-Materials Sci. Ed. 27 (5) (Oct. 2012) 861–865, https://doi.org/10.1007/s11595-012-0563-7.

[99] D. Liu, H. Ji, R. Peng, H. Cheng, C. Zhang, Infrared chameleon-like behavior from VO2(M) thin films prepared by transformation of metastable VO2(B) for adaptive camouflage in both thermal atmospheric windows, Sol. Energy Mater. Sol. Cells 185 (Oct. 2018) 210–217, https://doi.org/10.1016/j.solmat.2018.05.042.

[100] A. Frattolillo, G. Loddo, C.C. Mastino, R. Baccoli, Heating and cooling loads with electrochromic glazing in Mediterranean climate, Energy Build. 201 (Oct. 2019) 174–182, https://doi.org/10.1016/j.enbuild.2019.06.042.
[101] D. Liu, H. Cheng, X. Xing, C. Zhang, W. Zheng, Thermochromic properties of W-doped VO 2 thin films deposited by aqueous sol-gel method for adaptive infrared stealth application, Infrared Phys. Technol. 77 (Jul. 2016) 339–343, https://doi.org/10.1016/j.infrared.2016.06.019.
[102] N. Wang, et al., Terbium-doped VO $_2$ thin films: reduced phase transition temperature and largely enhanced luminous transmittance, Langmuir 32 (3) (Jan. 2016) 759–764, https://doi.org/10.1021/acs.langmuir.5b04212.
[103] X. Chen, Q. Lv, X. Yi, Smart window coating based on nanostructured VO2 thin film, Optik 123 (13) (Jul. 2012) 1187–1189, https://doi.org/10.1016/j.ijleo.2011.07.048.
[104] S. Taylor, Y. Yang, L. Wang, Vanadium dioxide based Fabry-Perot emitter for dynamic radiative cooling applications, J. Quant. Spectrosc. Radiat. Transf. 197 (Aug. 2017) 76–83, https://doi.org/10.1016/j.jqsrt.2017.01.014.
[105] S.-R. Wu, K.-L. Lai, C.-M. Wang, Passive temperature control based on a phase change metasurface, Sci. Rep. 8 (1) (Dec. 2018) 7684, https://doi.org/10.1038/s41598-018-26150-9.
[106] R. Sun, et al., Broadband switching of mid-infrared atmospheric windows by VO $_2$ -based thermal emitter, Opt Express 27 (8) (Apr. 2019) 11537, https://doi.org/10.1364/OE.27.011537.
[107] M. Tazawa, P. Jin, T. Miki, K. Yoshimura, K. Igrashi, IR Properties of SiO Deposited on V1yxWxO2 Thermochromic FIlms by Vacuum Evaporation, 2000, p. 4.
[108] M. Tazawa, P. Jin, S. Tanemura, Thin film used to obtain a constant temperature lower than the ambient, Thin Solid Films 281–282 (Aug. 1996) 232–234, https://doi.org/10.1016/0040-6090(96)08620-8.
[109] M. Ono, K. Chen, W. Li, S. Fan, Self-adaptive radiative cooling based on phase change materials, Opt Express 26 (18) (Sep. 2018) A777, https://doi.org/10.1364/OE.26.00A777.
[110] W.J.M. Kort-Kamp, S. Kramadhati, A.K. Azad, M.T. Reiten, D.A.R. Dalvit, "Passive radiative 'thermostat' enabled by phase-change photonic nanostructures, ACS Photonics 5 (11) (Nov. 2018) 4554–4560, https://doi.org/10.1021/acsphotonics.8b01026.
[111] A. Seeboth, R. Ruhmann, O. Mühling, Thermotropic and thermochromic polymer based materials for adaptive solar control, Materials 3 (12) (Dec. 2010) 5143–5168, https://doi.org/10.3390/ma3125143.
[112] T.-G. La, X. Li, A. Kumar, Y. Fu, S. Yang, H.-J. Chung, Highly flexible, multipixelated thermosensitive smart windows made of tough hydrogels, ACS Appl. Mater. Interfaces 9 (38) (Sep. 2017) 33100–33106, https://doi.org/10.1021/acsami.7b08907.
[113] H. Ye, X. Meng, L. Long, B. Xu, The route to a perfect window, Renew. Energy 55 (Jul. 2013) 448–455, https://doi.org/10.1016/j.renene.2013.01.003.
[114] T.S. Eriksson, E.M. Lushiku, C.G. Granqvist, Materials for radiative cooling to low temperature, Sol. Energy Mater. 11 (1984) 149–161.
[115] E.M. Lushiku, C.G. Granqvist, Radiative cooling with selectively infrared-emitting gases, J. Appl. Phys. 53 (8) (1982) 5526–5530, https://doi.org/10.1364/AO.23.001835.
[116] E.M. Lushiku, T.S. Eriksson, A. Hjortsberg, C.G. Granqvist, Radiative cooling to low temperatures with selectively infrared-emitting gases, Sol. Wind Technol. 1 (2) (1984) 115–121, https://doi.org/10.1016/0741-983X(84)90013-4.
[117] A. Hjortsberg, C.G. Granqvist, Radiative cooling with selectively emitting ethylene gas, Appl. Phys. Lett. 39 (6) (1981) 507–509, https://doi.org/10.1063/1.92783.
[118] H. Tian, S. Yang, Recent progresses on diarylethene based photochromic switches, Chem. Soc. Rev. 33 (2) (2004) 85, https://doi.org/10.1039/b302356g.